Supplement of The Cryosphere, 20, 2393–2416, 2026
https://doi.org/10.5194/tc-20-2393-2026-supplement
© Author(s) 2026. CC BY 4.0 License.

The Cryosphere Open Access EGU

Supplement of

Explicit representation of liquid water retention over bare ice using the SURFEX/ISBA-Crocus model: implications for mass balance at Mera glacier (Nepal)

Audrey Goutard et al.

Correspondence to: Audrey Goutard (audrey.goutard@univ-grenoble-alpes.fr)

The copyright of individual parts of the supplement might differ from the article licence.

S1 Crocus version used

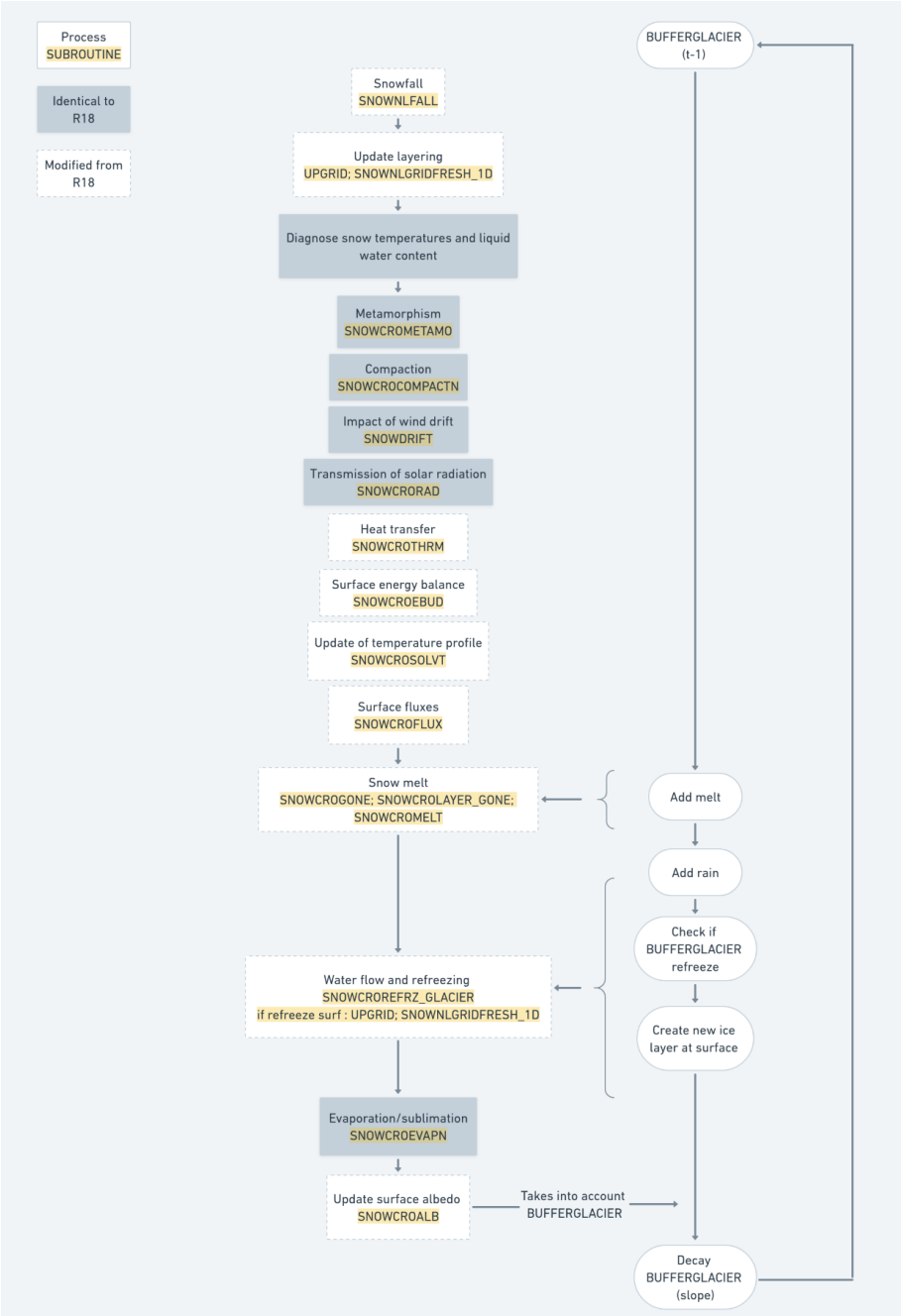

Figure S1: Crocus workflow with modified routines in white and unmodified routines in grey.

S2 Model calibration and evaluation

S2.1 Albedo

From the hourly observed and simulated albedo (simulation $BV_{default}$), daily values were computed by integrating over each day. Results are shown in Fig. S2, highlighting key surface state transitions such as snowfall events and bare ice periods. While this figure is not intended as a strict model validation, since ice albedo is one of the parameters used for calibration, it illustrates the challenges associated with selecting a representative value for ice albedo. Indeed, in Crocus, the albedo over ice surfaces is prescribed as a constant value, which does not capture its natural temporal variability. Observations at Mera Glacier show that ice albedo fluctuates significantly, typically ranging from 0.12 to 0.40, depending on seasonal conditions and surface state evolution. This variability is particularly evident during the monsoon season, as clearly shown from June to September of the 2021–2022 period in Fig. S2d. Given this variability, the fixed value of 0.35 used in this study represents a compromise that provides the best agreement with available observations. It also aligns well with the optimized value of 0.30 reported by Khadka et al. (2022), although slight differences remain. These discrepancies can be attributed to differences in model structure and, in particular, in the treatment of shortwave radiation penetration into snow and ice layers. This figure also highlights additional modeling challenges, especially during transitional periods marked by short snowfall events that temporarily cover the surface with snow, increasing albedo, but which rapidly disappear due to melt. These cases emphasize the uncertainties associated with the phase and amount of precipitation, as discussed in Section 5.1.1.

S2.2 Surface temperature

Fig. S3 presents a comparison between simulated (BV_{albedo} simulation) and observed daily mean surface temperature (ST) over the four study years. The results show a strong agreement between simulated and observed ST, with no systematic bias and a mean bias of 0.40°C (remaining below 0.8°C for each hydrological year). These results also demonstrate a very good agreement on the timing of the transition to temperate ice, which is a key process for evaluating the buffer effect investigated in this study. We selected ST as the primary evaluation variable because it serves as a direct indicator of the surface energy balance and determines whether the ice surface is temperate or cold, a critical factor influencing the buffer effect. Indeed, the buffer depends on the potential for melting and refreezing, which is directly governed by the available energy and therefore by surface temperature. The good agreement between model results and observations thus strengthens confidence in the model's ability to realistically represent the buffer effect.

S2.3 Annual mass balance

Simulated annual mass balances (MB) (BV_{albedo} simulation) are compared to MB measurements from the nearest stake located approximately 10–15 m from the AWS (GLACIOCLIM, https://glacioclim.osug.fr/). Results from the study performed by Khadka et al. (2022) using the COSIPY model are also reported (Table S1). A systematic bias of on average -1.37 m w.e. remains when comparing simulated MB with observations. However, the results are overall consistent with the findings of Khadka et al. (2022) (no systematic bias) except for the year 2021–2022. That study showed good agreement between observed and simulated glacier-wide MB, particularly with a good representation of mass balances compared to observations across elevation ranges. The bias between our simulations and the stake measurements

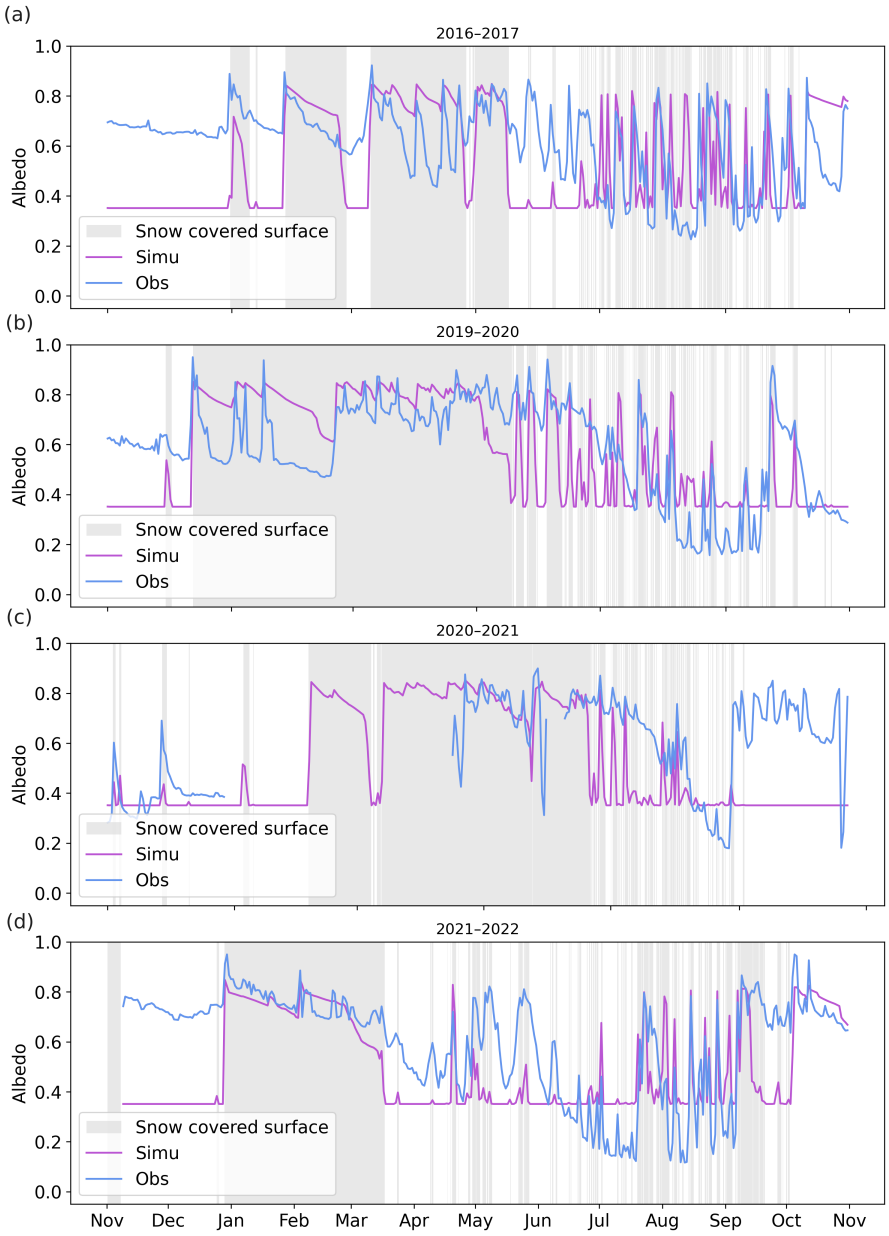

Figure S2: Evolution of simulated (purple) and observed (blue) daily albedo for different years. Observed and simulated albedo are computed as the daily mean over 24 hours, when valid measurements are available. Simulations were performed with Crocus $\mathrm{BV}_{\mathrm{default}}$ version. Grey areas indicate periods when the surface is covered with snow.

may partly be explained by local effects that are difficult to represent accurately in models. Indeed, our simulations were performed at a local point, while there is significant spatial variability in the study area. For instance, differences greater than 1 meter have been recorded between stakes located at the same elevation but on different parts of the glacier: one at the AWS, on the tongue of Naulek, and the other on the tongue of Mera, the main glacier tongue (see Fig. 1) (data available on the GLACIOCLIM website). Additionally, a well-known source of uncertainty in glacierized mountain catchments is the spatio-temporal representation of precipitation (amount and phase) in the observations (e.g., Intergovernmental Panel on Climate Change (IPCC), 2022), which has direct consequences on mass balance modeling uncertainties, especially at the local scale. This measurement uncertainty is even more challenging at Mera glacier, where the monsoon period is both a key accumulation and ablation

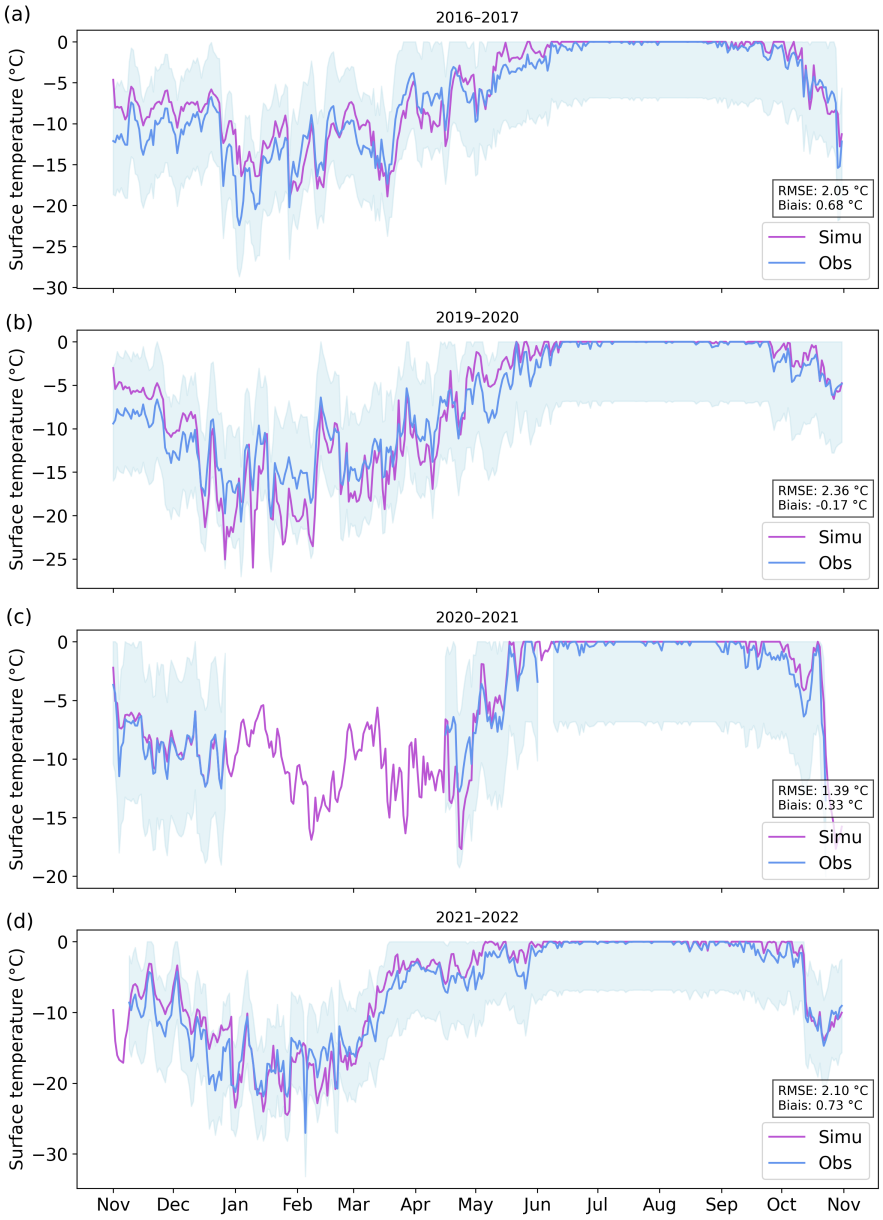

Figure S3: Evolution of simulated (purple) and observed (blue) daily surface temperature over the four study years. Simulations are performed using Crocus $BV_{default}$ configuration and observations are derived from the AWS longwave radiation measurements. The blue shaded area represents a 2.5% uncertainty (in K) corresponding to a 10% measurement uncertainty on LW.

period (Ageta and Higuchi, 1984). For that reason, several adjustments on precipitation amount and phase were tested (not shown), but they resulted in unrealistic surface dynamics, notably with inconsistent timing of snow vs. ice cover compared to observations. We therefore opted for a calibration that is in line with surface temperature measurements and a consistent albedo in order to reproduce realistic surface states (e.g., presence or absence of ice, temperate vs. cold surface), which are essential conditions for analyzing the modeled buffer behavior.

S2.4 Discussion and conclusion

Although we found good agreement between observed and simulated albedo, as well as surface temperature, two key indicators of surface energy balance, supporting the model's ability to realistically

Table S1: Simulated and observed annual mass balance (MB) at the AWS point, over the four study years. Simulated MB are from Crocus simulation ($BV_{default}$ version described in this study) and COSIPY simulations (Khadka et al. (2024)). The observed MB are from GLACIOCLIM measurements at the nearest stake located approximately 10–15 m from the AWS.

	2016-2017	2019-2020	2020-2021	2021-2022
Sim. MB (m w.e.) with Crocus $BV_{default}$	-3.17	-3.49	-3.24	-4.48
Sim. MB with Cosipy (from Khadka et al. (2024))	-3.56	-3.25	-3.66	-2.14
Obs. MB (GLACIOCLIM)	-2.14	-2.12	-0.72	-2.94

represent the buffer effect, it is important to emphasize that achieving realistic mass balance simulation is beyond the scope of this study. Mera Glacier is used here as a case study, and all comparisons aimed at quantifying the buffer effect are performed in a relative framework. In addition, this study is based on a large number of sensitivity tests, which serve two main purposes: first, to identify the key input variables that need to be well constrained for robust model performance; and second, to demonstrate that the conclusions regarding the significant influence of the buffer effect are not strongly dependent on specific input values (see Sect. 5.2). Our results show that even under extensive sensitivity tests on the most influential parameters, the buffer effect can have a substantial impact on surface processes.

S3 Layer strategy management and refrozen fraction

S3.1 Overview of layer management

The layer management strategy aims to maintain optimal discretization for heat diffusion resolution by preserving finer resolution near the surface while respecting constraints on the total number of layers (50 by default) and avoiding thickness variations of several orders of magnitude between successive layers.

When buffer refreezing occurs, the model must integrate the refrozen mass into the vertical discretization. The subroutine *upgrid_glacier* evaluates whether a new layer is formed or if the refrozen water is merged with an existing layer (see workflow in Appendix S1). This decision depends on the magnitude of the refrozen mass M_{refrz} and the current layer structure.

S3.2 Refreezing scenarios and layer creation

S3.2.1 Negligible refreezing

If M_{refrz} is lower than 3 J m^{-2} (equivalent to 1×10^{-8} m), it is added to the first layer without further updates to other variables, to avoid numerical instabilities associated with extremely thin layers.

S3.2.2 Layer aggregation

If the potential new layer would be thinner than 1/10 of the first layer thickness, M_{refrz} is aggregated into the existing surface layer. This maintains a reasonable vertical discretization and avoids creating excessively thin layers that would compromise numerical stability.

S3.2.3 New layer creation

If the refrozen mass is thick enough (greater than 1/10 of the first layer thickness) and the total number of layers in the model is below the maximum limit (50 layers by default), a new refrozen ice layer is created at the surface with temperature T_0 (273.15 K) and a density of 917 kg m^{-3}.

S3.2.4 Layer creation with column reorganization

If the model has already reached the maximum number of layers, it first identifies two similar layers within the column (based on temperature and density proximity) and merges them. This creates space for the new refrozen ice layer, which is then added at the surface at temperature T_0 with density 917 kg m^{-3}.

S3.3 Continuous layer management

Even when refreezing occurs slowly, the surface layer thickness remains controlled because the *upgrid* routine is called at the start of each time step (see workflow in Appendix S1). This routine automatically subdivides layers that become too thick relative to adjacent layers, ensuring consistent discretization throughout the simulation.

S3.4 Refreezing fraction calculation

S3.4.1 Definition and purpose

The albedo of the first and/or second layer must be updated when buffer refreezing occurs. Because refreezing can either form a new layer or aggregate with an existing one, a refreezing fraction variable $r_{frac,i}$ is introduced to track the proportion of refrozen ice within layers $i \in [1, 2]$. This variable varies between 0 (bare ice) and 1 (fully refrozen ice) and is used to compute the layer albedo as a weighted average between bare ice and refrozen ice albedo values.

S3.4.2 Calculation formulas

The refreezing fraction is calculated differently depending on whether a new layer is created or the refrozen mass is aggregated:

$$\begin{cases} \text{if creation of new layer: } \begin{cases} r^+_{frac,2} = r^-_{frac,1} \\ r^+_{frac,1} = 1 \end{cases} \\ \text{if aggregation to existing layer: } r^+_{frac,1} = \dfrac{z_{refrz} + r^-_{frac,1} z_1}{z_{refrz} + z_1} \end{cases} \tag{S1}$$

where z_1 (in m) is the thickness of the first layer and z_{refrz} (in m) is the thickness of refreezing, computed as:

$$z_{refrz} = \frac{M_{refrz}}{L_m \rho_i} \tag{S2}$$

where L_m is the latent heat of fusion for ice and $\rho_i = 917$ kg m^{-3} is the ice density.

S3.4.3 Temporal evolution and reset conditions

The variable $r_{frac,i}$ is maintained from one time step to the next to preserve information about refreezing for albedo calculations. When melting occurs in layer i, $r_{frac,i}$ is reset to 0, based on the hypothesis that the refrozen layer at the surface melts first. The refreezing fraction is also updated whenever changes in layering occur (aggregation or separation of layers) according to the scenarios detailed below.

S3.5 Additional layering scenarios affecting r_{frac}

S3.5.1 Surface regrid (layer 1 aggregation)

Surface regridding occurs when the first layer becomes too thin and must be aggregated with the second layer. The new first layer thickness becomes:

$$z^+_1 = z^-_1 + z^-_2 \tag{S3}$$

The refreezing fractions are aggregated using depth-weighted averaging:

$$\begin{cases} r^+_{frac,1} = \dfrac{z^-_1 r^-_{frac,1} + z^-_2 r^-_{frac,2}}{z^-_1 + z^-_2} \\ r^+_{frac,2} = 0 \end{cases} \tag{S4}$$

S3.5.2 Splitting of layer 2

Layer splitting occurs when layer 2 exceeds the maximum thickness threshold and must be divided into two layers. The layer is split into equal thicknesses:

$$\begin{cases} z_2^+ = \frac{1}{2} z_2^- \\ z_3^+ = \frac{1}{2} z_2^- \end{cases} \tag{S5}$$

When layer 2 splits, the refrozen fraction is divided equally between the two new layers. Since r_{frac} is only defined for layers 1 and 2, the new layer 2 retains half of the original fraction while layer 3 receives no fraction:

$$\begin{cases} r_{frac,2}^+ = \frac{1}{2} r_{frac,2}^- \\ r_{frac,1}^+ = r_{frac,1}^- \end{cases} \tag{S6}$$

S3.5.3 Splitting of the first layer

First layer splitting occurs when the surface layer exceeds the maximum thickness threshold. An optimal thickness value $z_{1,\text{opti}}$ is calculated based on column-wide optimization principles. The new layer thicknesses are:

$$\begin{cases} z_1^+ = 1.5 z_{1,\text{opti}} \\ z_2^+ = z_1^- - z_1^+ \end{cases} \tag{S7}$$

The refrozen fractions are redistributed using depth-based weighting:

$$\begin{cases} r_{frac,1}^+ = \frac{z_1^+}{z_1^-} r_{frac,1}^- \\ r_{frac,2}^+ = \left(1 - \frac{z_1^+}{z_1^-}\right) r_{frac,1}^- \end{cases} \tag{S8}$$

S3.5.4 Aggregation of layer 2 with layer 3

Layer aggregation occurs when layer 2 requires regridding and must be combined with layer 3. The new layer 2 depth becomes:

$$z_2^+ = z_2^- + z_3^- \tag{S9}$$

Layer 1 remains unchanged while layer 2 receives a weighted fraction based on the original depth of layer 2:

$$\begin{cases} r_{frac,1}^+ = r_{frac,1}^- \\ r_{frac,2}^+ = \frac{z_2^-}{z_2^- + z_3^-} r_{frac,2}^- \end{cases} \tag{S10}$$

S3.5.5 Melt reset

When melting occurs in layers 1 and/or 2, the process initiates at the surface. This surface melting removes the refrozen ice, returning the affected layers to bare ice conditions. Consequently, the refrozen

fraction resets to zero:

$$r^{+}_{frac,i} = 0 \tag{S11}$$

for layer i where melting occurs.

S4 Mass balance for BV_{albedo} in 2021-2022

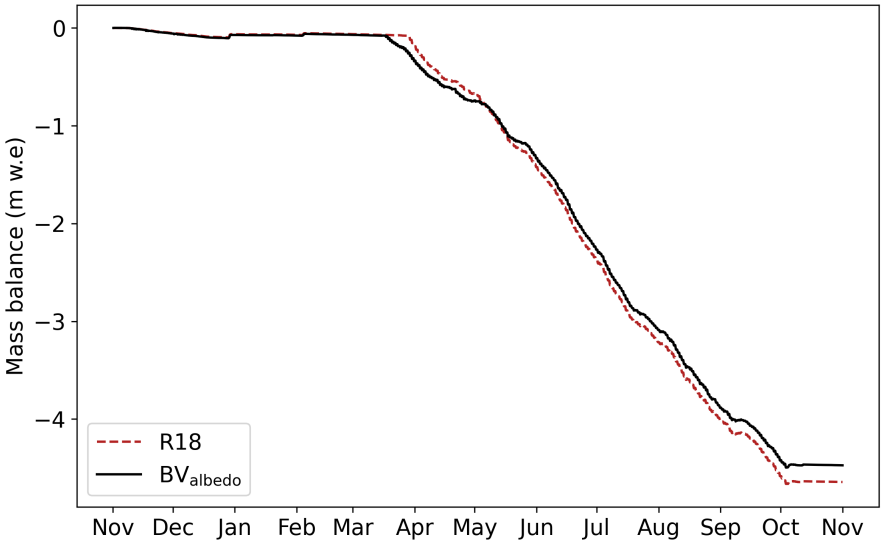

Figure S4: Simulated seasonal mass balance evolution (in m w.e.) for 2021–2022 at Mera Glacier. Solid black line is BV_{albedo} and dashed line is R18.

S5 Surface state

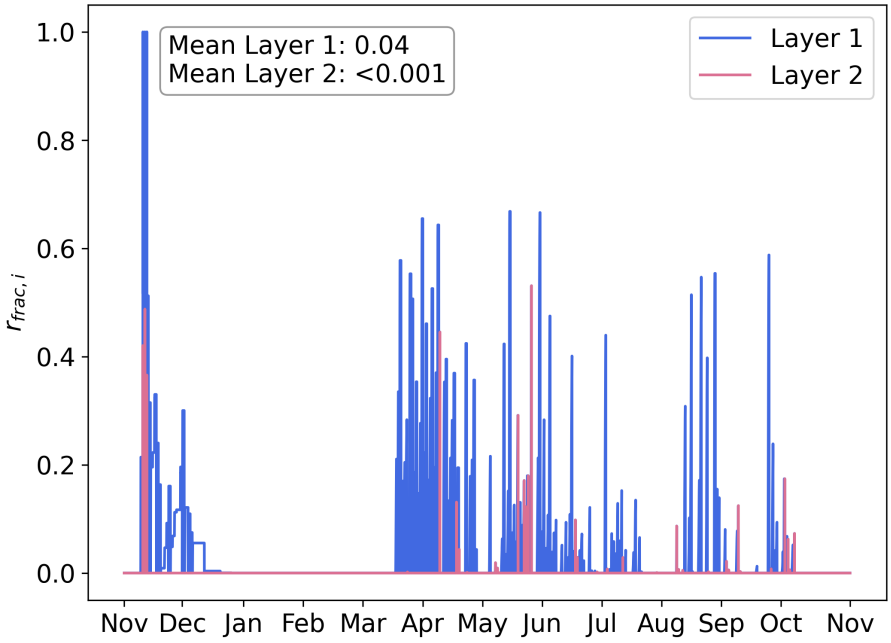

Figure S5: Evolution of layers 1 in blue and 2 in purple refreezing fraction $r_{frac,i}$ for 2021-2022. Simulation performed using default parameters (D=0.995, $z_{max,buff}$=0.01, x=0.2, albedo of liquid water, bare ice and refrozen ice at 0.35).

References

Ageta, Y. and Higuchi, K.: Estimation of Mass Balance Components of a Summer-Accumulation Type Glacier in the Nepal Himalaya, Geografiska Annaler: Series A, Physical Geography, 66, 249–255, https://doi.org/10.1080/04353676.1984.11880113, 1984.

Intergovernmental Panel on Climate Change (IPCC): The Ocean and Cryosphere in a Changing Climate: Special Report of the Intergovernmental Panel on Climate Change, Cambridge University Press, ISBN 9781009157971, https://doi.org/10.1017/9781009157964, 2022.

Khadka, A., Wagnon, P., Brun, F., Shrestha, D., Lejeune, Y., and Arnaud, Y.: Evaluation of ERA5-Land and HARv2 Reanalysis Data at High Elevation in the Upper Dudh Koshi Basin (Everest Region, Nepal), Journal of Applied Meteorology and Climatology, 61, 931–954, https://doi.org/10.1175/JAMC-D-21-0091.1, publisher: American Meteorological Society Section: Journal of Applied Meteorology and Climatology, 2022.

Khadka, A., Brun, F., Wagnon, P., Shrestha, D., and Sherpa, T. C.: Surface energy and mass balance of Mera Glacier (Nepal, Central Himalaya) and their sensitivity to temperature and precipitation, Journal of Glaciology, pp. 1–22, https://doi.org/10.1017/jog.2024.42, 2024.